Fish and Shellfish Immunology 92 (2019) 151–164

Contents lists available at ScienceDirect

Fish and Shellfish Immunology

journal homepage: www.elsevier.com/locate/fsi

Full length article

Analyses of the gene structure and function of olive flounder (*Paralichthys olivaceus*) interleukin 12 (IL-12)

Daniel Kim[a,1,4], Soon Ho Lee[a], Hayoung Lee[a,2], Seong-jung Kim[a,3], Kwan Hee Lee[b], Seong Kyu Song[a,*]

[a] School of Life Science, Handong University, 558 Handong-ro, Pohang-city, Gyeongbuk, 37554, South Korea
[b] Immunus (Co. Ltd.) Nehemiah hall Rm. 301, Handong University, 558 Handong-ro, Pohang-city, Gyeongbuk, 37554, South Korea

ARTICLE INFO

Keywords:
IL-12p35
IL-12p40
Single chain IL-12
Functional IL-12
Olive flounder

ABSTRACT

IL-12 is an important cytokine that connects the innate and adaptive immune systems. The complete gene structure of olive flounder IL-12 and its characteristics have not yet been formally reported. Here, we report the complete sequences of both subunits of olive flounder *IL-12* (*IL-12p35* and *IL-12p40*). In addition, its function was analyzed by generating the single-chain rIL-12 of which subunits were fused by a GS linker and the rIL-12-specific mouse antibody. The cDNA sequences of *IL-12p35* and *IL-12p40* were 1059 nucleotides and 1319 nucleotides, respectively. The analyses of their gene structures, deduced amino acid sequences, protein model structures, and phylogenetic trees confirmed the accurate identification of olive flounder IL-12. The protein structure model suggested that an inter-subunit disulfide bond might be formed between the Cys177 of p35 and Cys74 of p40 to link the subunits. Olive flounder expressed *IL-12p40* at higher levels than *IL-12p35* in the various tissues under natural conditions although both expression levels were low. However, when infected by *Edwardsiella tarda* or stimulated by LPS, the flounder expressed both of the subunit genes at similar maximized levels in 6 h and gradually reduced thereafter. Olive flounder PBMC induced with the rIL-12 increased *IFN-γ* and *TNF-α* expression but decreased *IL-10* expression as did treatment with LPS. However, when the LPS-treated PBMC were neutralized with the rIL-12-specific antibody, the pattern of cytokine expression was precisely reversed. In conclusion, we have formally identified the gene structure and function of olive flounder IL-12.

1. Introduction

Interleukin-12 (IL-12) is a pro-inflammatory cytokine mainly produced by activated innate immune cells such as macrophages, dendritic cells, and B cells [1,2]. IL-12 links the innate and adaptive immune responses by inducing IFN-γ production from T cells and NK cells [3,4]. Many stimulants like LPS induce *IL-12* gene expression by activating the TLR4-mediated JAK-STAT signaling pathways [2,4–7]. IL-12 acts on T and NK cells resulting in proliferation, differentiation, and production of cytokines including IFN-γ. Activated naïve $CD4^+$ T cells differentiate into Th1, Th2, and Th17 cells depending on the local environment such as the availability of the kinds of cytokines. IL-12 stimulates naïve $CD4^+$ T cells to differentiate into Th1 cells, a significant IFN-γ producer [6,12,13]. The IFN-γ produced by Th1 cells and NK cells, in turn, activates innate immune cells to secrete IL-12 in a positive feedback manner, enhancing cell-mediated immune responses [8–11]. However, this positive feedback loop can also cause severe pathology such as septicemia if the loop is not adequately controlled [32,33].

IL-12 is a heterodimer of IL-12p35 and IL-12p40, which are linked by a disulfide bond to form a biologically active IL-12p70 [1,8,9,13–16,24,26]. The IL-12p35 is a subunit used only for IL-12. However, the IL-12p40 serves as both subunits of IL-12 and IL-23 [29,41]. Under unstimulated conditions, innate immune cells constitutively express both IL-12p35 and IL-12p40 subunit mRNAs at low levels. However, *IL-12p35* is expressed at higher levels than *IL-12p40* [2,17]. Although the functions of IL-12 in immune regulation have been

* Corresponding author.
E-mail address: sksong@handong.edu (S.K. Song).
[1] Current address: KIGAM, Korea Institute of Geoscience and Mineral Resources, 905, Yeongilman-daero, Heunghae-eup, Buk-gu, Pohang-si, Gyeongbuk, 37559, South Korea.
[2] Current address: Department of Bio-Analytical Science, University of Science and Technology, Daejeon, 34113, South Korea.
[3] Current address: School of Life Sciences, Ulsan National Institute of Science and Technology, Ulsan 44919, South Korea.
[4] Daniel Kim and Soon Ho Lee contributed equally to this article.

https://doi.org/10.1016/j.fsi.2019.05.033
Received 15 January 2019; Received in revised form 13 May 2019; Accepted 17 May 2019
Available online 18 May 2019

extensively studied in mammals, similar studies are lacking in fish. Most of the IL-12 studies in teleost are limited to the identification of *IL-12* gene sequences and their isoforms: pufferfish (*Takifugu rubripes*) [18], sea bass (*Dicentrarchus labrax*) [18], common carp (*Cyprinus carpio*) [20], Atlantic salmon (*Salmo salar*) [30], rainbow trout (*Oncorhynchus mykiss*) [37], zebrafish [38], Japanese amberjack (*Seriola quinqueradiata*) [27], and green spotted puffer (*Tetraodon nigroviridis*) [28].

Olive flounder is one of the most economically significant cultured fish in Korea, Japan, and China. However, the *IL-12* gene sequences of olive flounder and its immune modulatory function have not yet been explored, which may be essential for designing effective vaccines. In this article, we report the gene sequences and structure of olive flounder *IL-12*. Its immunological functions were studied by constructing the functional single-chain rIL-12 and the anti-olive flounder rIL-12 mouse antibody.

2. Materials and methods

2.1. Cloning of full-length mRNA sequences of olive flounder IL-12p35 and IL-12p40 subunits

2.1.1. Total RNA extraction

For induction of *IL-12p35* and *IL-12p40* expression, olive flounder weighing ~50 g was intraperitoneally injected with 1 μg of LPS (Sigma-Aldrich, USA) for 6 h. The fish was sacrificed, and the head kidney and spleen were extracted and stored in RNA*later*™ Stabilization Solution (Ambion, USA) solution at 4 °C overnight. Total RNA was isolated from the tissues using RNeasy Plus Mini Kit (Qiagen, USA) following the manufacturer's instructions with minor modification; 25 mg of each tissue was homogenized in 500 μl lysis buffer with IKAT 10 Basic Ultra Turrax Homogenizer (IKA, USA). Two independent batches of the first-strand cDNA were synthesized with 5 μg of RNA using SuperScriptTM III Reverse Transcriptase (Invitrogen, USA) following the product manual.

2.1.2. Initial determination of partial mRNA sequences

Conserved sequences of teleost *IL-12p35* and *p40* were identified by analyzing the nucleotide database of the National Center for Biotechnology Information (NCBI). The reference nucleotide sequences for *IL-12p35* and *p40* were Atlantic halibut (*Hippoglossus hippoglossus*, FJ769831.1), Nile tilapia (*Oreochromis niloticus*, XM_025898369.1, XM_019364048.2), Atlantic salmon (*Salmon salar*, BT049114.1, HG917954.1), and rainbow trout (*Oncorhynchus mykiss*, HE798541.1, HE798542.1). Through multiple sequence alignment using ClustalX [21], several primers potentially able to amplify the sequences of putative olive flounder *IL-12p35* and *IL-12p40* were generated (Table 1).

The primer sets were tested to determine whether they were able to amplify putative olive flounder *IL*-12 by RT-PCR analysis. The PCR was performed using ExTaq (TaKaRa, Japan) in a total volume of 50 μl at 94 °C for 5 min; 35 cycles of 94 °C for 45 s, 62 °C for 45 s, and 72 °C for 45 s; final extension at 72 °C for 10 min. The PCR products were TA-cloned using a T-Blunt™ PCR Cloning Kit (Solgent, South Korea) and then both strands were sequenced by Solgent Co. Ltd., using a 3730XL DNA Analyzer (ABI, USA). The initial sequences obtained, 555 base pairs of tentative *IL-12p35* and 591 base pairs of tentative *IL-12p40*, were further validated using BLAST [22].

2.1.3. Cloning of the full-length cDNA of olive flounder IL-12p35 and IL-12p40

cDNA was prepared using a SMARTer® RACE cDNA Amplification Kit (Clontech, USA) using 1 μg of RNA, 5′-CDS Primer A, and 3′-CDS Primer, according to the manufacturer's instructions. Primary PCR reactions were performed with universal primer A mix (UPM, supplied in the SMARTer® RACE cDNA Amplification Kit). Primers used for the reaction were: p35_F2 for p35 3′-RACE, p35_R2 for p35 5′-RACE, p40_F2 for p40 3′-RACE, and p40_R2 for p40 5′-RACE. The primary PCR products were then used as templates for nested PCR using primers: p35_F3, p35_R3, p40_F3, p40_R3, and nested universal primer A (supplied by the manufacturer). All steps were performed in a total volume of 25 μl: the initial step was performed in 20 cycles of 94 °C for 45 s then 72 °C for 45 s; the second step was performed in 15 cycles of 94 °C for 45 s, 62 °C for 45 s, then 72 °C for 45 s with a final extension at 72 °C for 10 min. The primers used for RACE PCR are listed in Table 1.

2.2. Sequencing of genomic DNA (gDNA) and determination of the gene structures of IL-12

Olive flounder gDNA was extracted from tissues preserved in RNA*later*® Stabilization using G-spin™ Total DNA Extraction Mini Kit (iNtRON Biotechnology, South Korea). The genomic loci of olive flounder *IL-12p35* and *IL-12p40* were determined using a primer walking method, using a 3730XL DNA Analyzer (ABI, USA). The gene structural schema of the *IL-12p35* and *IL-12p40* genes was determined by inputting the gDNA and mRNA sequences into Exon-Intron Graphic Maker by Nikhil Bhatla (http://wormweb.org/exonintron). Three different nucleotide sequences of teleost *IL-12p35* and *IL-12p40* were used as the references of the study: European bass (*Dicentrarchus labrax*, p35: 038.1, p40: DQ388040.1), rainbow trout (*Oncorhynchus mykiss*, p35: HE798541.1, p40: HE798542.1) and Japanese puffer (*Takifugu rubripes*, p35: AB096267.1, p40: AB096268.1).

2.3. Analyses of amino acid sequence, multiple sequence alignment, and phylogenetic tree of olive flounder IL-12

Deduced amino acid sequences of IL-12p35 and IL-12p40 were aligned with those of other bony fish, mouse, and human using the Cluster W2 – Multiple Sequence Alignment (http://www.ebi.ac.uk/Tools/msa/clustalw2/). The EMBL accession numbers for IL-12p35 were: human (*Homo sapiens*, AF101062.1); mouse (*Mus musculus*, BC116855.1); European seabass, DQ388037.1; orange-spotted grouper (*Epinephelus coioides*, HQ154062.1); grass carp (*Ctenopharyngodon idella*, KF944667.1); and rainbow trout, HE798541.1. The accession numbers for IL-12p40 were: human, AF180563.1; mouse, NM_008352.2; common carp, AJ628699.1; striped beakfish (*Oplegnathus fasciatus*, KJ143630.1); rainbow trout, AJ548830.1; and Atlantic halibut, FJ769831.1. The protein domains of olive flounder IL-12 were predicted using the Simple Modular Architecture Reach Tool (SMART) (http://smart.embl-heidelberg.de/). The phylogenetic tree of the IL_12 was constructed by the neighbor-joining method using MEGA6.0 (http://www.megasoftware.net) and was bootstrapped 1000 times.

2.4. Structural modeling of olive flounder IL-12

The structural model of olive flounder IL-12 was constructed based on the human IL-12 crystal structure, 1F45 [23], using Discovery Studio 4.1 (3DS BIOVIA Inc.). Modeling was performed following the manufacturer's Build Homology Models protocol and further refined with loop refinement (MODELER).

2.5. Expression profiles of IL-12 at olive flounder tissues in natural and stimulated conditions by LPS or E. tarda infection

Tissue samples for control were collected from three fish before stimulation by LPS or *E. tarda* infection; hindgut, foregut, liver, spleen, head kidney, trunk kidney, gill, and blood samples were obtained. Twenty-one fish weighing 100 ± 2.7 g were injected *i.v.* with 1 μg of LPS (Sigma, USA) in 100 μl/fish through a caudal vein. At each specific time point (3, 6, 9, 12, 24, or 48 h post-injection), three fish were sacrificed, and the head kidneys were aseptically removed. The isolated specimens were immediately immersed in RNA*later*® Stabilization

Table 1
Primers used in the study. Abbreviations: A, adenosine; T, thymidine; G, guanosine; C, cytidine; F, forward; R, reverse.

Gene	Primers	Sequence (5' - 3')	Use
IL-12p40	P40_F1	GGAGAGTACAGCTGCTGG	Sequence retrieval
	P40_R1	GTCTCTGGAGCGAACCCT	Sequence retrieval
	P40_F2	AGGGTCCGCTCCAGAGACTCG	3′-RACE
	P40_F3	TGCTCTCAACCTGGAGCAATTGG	3′-RACE
	P40_R2	CGTCCTGCTGGATATTATCCTCCA	5′-RACE
	P40_R3	TTGCAGGTCAGTGTGACTGCGTC	5′-RACE
	P40_qF1	CTCTCCCTACGCCGAGGAAA	qRT-PCR
	P40_qR1	GCTAATCTGGGGACTGTCGG	qRT-PCR
	BamHI_P40F	GTTTGGATCCCTTGACCGCTTTCCAGAAAATGTTG	Cloning
	P40R_linker	GGACTCCTTGGAAAAATGTAACCAAC GGTGGCGGTGGCTCGGGTGGCGGTGGCTCGGGTGG	Cloning
IL-12p35	P35_F1	TGGCGCACATCCACAGGACTC	Sequence retrieval
	P35_R1	CTTCCTGTGGTCTCCTGAGGCG	Sequence retrieval
	P35_F2	GCACTTCTGAGCCCAACTCTGGG	3′-RACE
	P35_F3	CGCCTCAGGAGACCACAGGAAG	3′-RACE
	P35_R2	CCCAGATTGGGCTCAGAAGTGC	5′-RACE
	P35_R3	GGACTTCTGAGTGGGGACTTGAGG	5′-RACE
	P35_qF1	CTGCTCCCTGATGCCGAATG	qRT-PCR
	P35_qR2	CAGCTCGGTTGATGGTGATC	qRT-PCR
	Linker_P35F	GCTCGGGTGGCGGTGGCTCGGGTGGCGGTGGCTCGCTCCCGCTGAGGACAGACAAT	Cloning
	P35R_stop_XhoI	CTCGAGTCACTTCCTGTGGTCTCCTGAGGCG	Cloning
IFN-γ	IFN-γ_qF1	CAGGAGCTGAGGACAAATCG	qRT-PCR
	IFN-γ_qR1	GAACTCGCCTCCTCGTACAT	qRT-PCR
TNF-α	TNF-α_qF1	CGGCCATCCATTTAGAAGGT	qRT-PCR
	TNF-α_qR1	GGGATGATGATGTGGTTGTC	qRT-PCR
β-actin	β-actin_qF1	TGCAGAAGGAGATCACAGCC	qRT-PCR
	β-actin_qR1	ACTCCTGCTTGCTGATCCAC	qRT-PCR

Solution overnight at 4 °C and kept at −80 °C until use.

E. tarda was freshly grown overnight in brain heart infusion (BHI) medium and resuspended in PBS to 1×10^5 CFU/μl. Twenty-one fish were injected *i.v.* with *E. tarda* at 1×10^5 CFU/g body weight via a caudal vein. Tissue samples were collected and stored in the same manner as the LPS-treated fish.

2.6. Real-Time quantitative PCR (qRT-PCR) analysis

qRT-PCR was performed in a 20 μl volume (cDNA 10 ng/rxn) using SYBR® Premix Ex Taq™ II (Tli RNase H plus) (TAKARA, Japan) and a StepOnePlus Real-Time PCR System (Applied Biosystems, USA), according to the manufacturers' instructions. The primers used in the qRT-PCR are listed in Table 1. The level of *β-actin* gene expression was used as an internal control to normalize the relative gene expression of samples. Relative fold expression was analyzed with the 2-ΔΔCT method described by Livak and Schmittgen [25].

2.7. Generation of a functional single-chain olive flounder rIL-12

IL-12 is biologically active only when its IL-12p35 and IL-12p40 subunits are linked by a disulfide bond. In order to generate a functional olive flounder rIL-12, the cDNAs of *IL-12p35* and *IL-12p40* subunits were fused using a flexible glycine-serine linker forming a single chain.

2.7.1. Production of a single-chain olive flounder IL-12 cDNA by connecting the subunit cDNAs, IL-12p35 and IL-12p40

Olive flounder *IL-12p35* and *IL-12p40* cDNA were amplified using specific primers [p35: Linker_P35F – P35R_stop_XhoI; p40: BamHI_P40F – P40R_Linker] (Table 1). The PCR was performed using ExTaq (TaKaRa, Japan) in a 50 μl volume at 94 °C for 5 min; 35 cycles of 94 °C for 60 s, 60 °C for 60 s, and 72 °C for 60 s; final extension at 72 °C for 10 min. The PCR products were electrophoresed in 1% agarose gel and purified using the AccuPrep® Gel Purification Kit (Bioneer, Daejeon, Korea). Then, overlap-extension PCR was performed to produce the single-chain olive flounder *rIL-12* with an approximately equal number of *IL-12p35* and *IL-12p40* cDNA molecules and primers [BamHI_P40F – P35R_stop_XhoI] (Table 1).

2.7.2. Cloning of the single-chain olive flounder rIL-12 to an expressing vector

The single-chain olive flounder *rIL-12* PCR product was initially cloned into the TA vector using a T-Blunt™ PCR Cloning Kit (Solgent, South Korea). The insert was then transferred to an expression vector, the pProex HTb plasmid, at the BamHI and XhoI restriction sites using T4 DNA ligase (Promega, USA).

2.7.3. Expression and purification of the single-chain olive flounder rIL-12

Olive flounder rIL-12 was expressed in *E. coli* BL-21 cells and verified by western blot analysis. The *E. coli* BL-21 cells harboring the rIL-12 plasmid were induced with 400 μM IPTG at 0.6 OD_{600} for 4 h at 37 °C. The bacteria were collected by centrifugation at 5000 g for 10 min at 4 °C, and the pellet was washed twice with PBS and lysed by sonication (Sonifier, Branson, USA) for 2 min for 30 cycles. The lysate was diluted in 8 M urea buffer (8 M urea dissolved in 1x PBS) and then centrifuged at 13,000 rpm for 10 min at 4 °C. The supernatant was kept at 4 °C until use. Briefly, the supernatant was electrophoresed in a 10% SDS-PAGE gel after dilution with 5X SDS sample buffer (250 mM Tris-HCl, 0.5 M DTT, 10% SDS, 0.25% bromophenol blue, 50% glycerol, pH 6.8). Two identical gels were prepared with the same sample: one for the Coomassie blue staining and the other for western blot analysis. For western blot analysis, the gel was transferred onto a PVDF membrane (Millipore, USA) followed by blocking with 5% skim milk (BD, USA) containing TBS-T (10 mM Tris-HCl, 15 mM NaCl, 0.05% Tween®-20, pH 7.5) solution. The primary antibody was 1:2000 diluted mouse anti-6xHis Tag antibody (Bio-legend, USA) and the secondary antibody was 1:4000 diluted HRP-conjugated goat anti-mouse IgG antibody (Bioss Inc, USA). The primary antibody was added to the TBS-T solution containing 3% skim milk and incubated overnight at 4 °C. Following the secondary antibody treatment, the solution was further incubated for 1.5 h at 25 °C. The membrane image of the western blot was developed using 1:10 diluted SuperSignal Femto Substrate (Thermo, USA) and an Omega LumG Imager (Aplegen, USA) according to the manufacturers' instructions.

Olive flounder rIL-12 was purified by gravity flow using Ni-NTA

(A)

cDNA sequence of *Paralichthys olivaceus IL-12p35*

```
1    accgggctccaccacagatttctatctgagcagagacATGGCCAACTTTCATTTGTACCTCGCCAGCTGTGCGCTGCTGCTGACGCTCGG
                                          M  A  N  F  H  L  Y  L  A  S  C  A  L  L  L  T  L  G   18
91   GTGGCGCACATCCACAGGACTCCCGCTGAGGACAGACAATTGCGCACAGTGCGCACTGCTCTTCAAGGGCCTTCTGCTCAACATCACGGA
       W  R  T  S  T  G  L  P  L  R  T  D  N  C  A  Q  C  A  L  L  F  K  G  L  L  L  N  I  T  E   48
181  GCTTCTGGACAACGATATTTTGTGTTATGGCATCACATCGGATAAGGTGGTGGTGAGGAGTAAAGCTGAGACTTCACTCGCCTGCGCACC
       L  L  D  N  D  I  L  C  Y  G  I  T  S  D  K  V  V  V  R  S  K  A  E  T  S  L  A  C  A  P   78
271  CACTCTCACTCAGAACTCAAGCTGCATGATGCAAAGAAATTCGCCCTTTAGTGAGAGTGAATGTTTGATGAACATCATGAAGGACTTGGT
       T  L  T  Q  N  S  S  C  M  M  Q  R  N  S  P  F  S  E  S  E  C  L  M  N  I  M  K  D  L  V  108
361  TTACTATGACGCTGCTATTAGTTCTTACCTCAAGTCCCCACTCAGAAGTCCAGAAGAAGAAGTTGCACTTCTGAGCCCAACTCTGGGAAT
       Y  Y  D  A  A  I  S  S  Y  L  K  S  P  L  R  S  P  E  E  E  V  A  L  L  S  P  T  L  G  I  138
451  AATAAAGAGCTTGAAGAACTGCTCCCTGATGCCGAATGAAGAGAATGACACCTCAGAGGAGGACGTTGCTCAGATGTGGGGGAGCGACAC
       I  K  S  L  K  N  C  S  L  M  P  N  E  E  N  D  T  S  E  E  D  V  A  Q  M  W  G  S  D  T  178
541  CTACACTAACAGACAGGAGATGTGCAAGATGATGAGAGGCTTCTATGTCCGAACGATCACCATCAACCGAGCTGTGGGCTACATCGCCTC
       Y  T  N  R  Q  E  M  C  K  M  M  R  G  F  Y  V  R  T  I  T  I  N  R  A  V  G  Y  I  A  S  208
631  AGGAGACCACAGGAAGTAAtcaacctgcagcctcatcatcatcaccatcattccaatcagtgccacagaatctcctttaaatcattgcaa
       G  D  H  R  K  *                                                                          213
721  ctttgcaaaatcttcttgatcattcactaccatcacttgtacctacaactactgaccaaatagttcgtcacactgtacatgatgcaccac
811  tgtcagcatggttattgctcagacataaactaagctgacttgatgccagtctcatcacccagtgagagctgaaagagtcaacctcttgcc
901  aagtttagcagtggaggccatgttggccttttatacatatgaatgtaatccaatatttggggtaatgtatctatttatgaatatattta
991  ttaattctatttatttgatggcctgtgatgttatttattgaaattgaataataagtatttttttggta
```

(B)

cDNA sequence of *Paralichthys olivaceus IL-12p40*

```
1    aaaggggctgtggtgatggtgatgatgatgatgatgcatgctgtacgcaagatataaaaatgaggctcagtgggcagtgagagcaaacaa
91   tcggcaggattccttcaactggacctccgctcttgatttttcagcatcacttgagcgtaatttcagccaaatgATGACTCTGTCTTTGTG
                                                                          M  T  L  S  L  W    6
181  GAAATTTGGACTTCTGCTCATTAGCTTCATAGGAGCAAATGGACTTGACCGCTTTCCAGAAAATGTTGTGGCAAAAAGGAATGACGCAGT
       K  F  G  L  L  L  I  S  F  I  G  A  N  G  L  D  R  F  P  E  N  V  V  A  K  R  N  D  A  V   36
271  CACACTGACCTGCAACACAAACACTGACGGAGCAGTCACGTGGAGGTTTGACGGTGAAGTGATGGAGGATTTGGAGGATAATATCCAGCA
       T  L  T  C  N  T  N  T  D  G  A  V  T  W  R  F  D  G  E  V  M  E  D  L  E  D  N  I  Q  Q   66
361  GGACGGTCAAAATCTGAGCTTGACAGAAGTGGATACCCCCATACTGGGAGAGTACAGCTGCTGGAGAGGAAGAGAGATGTTGTCATCGAC
       D  G  Q  N  L  S  L  T  E  V  D  T  P  I  L  G  E  Y  S  C  W  R  G  R  E  M  L  S  S  T   96
451  CTACCTGCTGCTGGAGGCTGAGGAGGAAGAGGAATTAGATACCAGCATCAATTGTTGGGCAAAGTCGTATCACTGTAACTTCAGCTGCAT
       Y  L  L  L  E  A  E  E  E  E  E  L  D  T  S  I  N  C  W  A  K  S  Y  H  C  N  F  S  C  I  126
541  CTGGAAAGACAGCAGAATCAAAGCAGGTCGCCTTGGACTGGGCCATGGCTGCACTGAAGGTGGGAAGTTGTGTCACTGGGTCAGCAGCAG
       W  K  D  S  R  I  K  A  G  R  L  G  L  G  H  G  C  T  E  G  G  K  L  C  H  W  V  S  S  S  156
631  TGATCAGATCCCGGGTGGGGGATTTCAGTTTGAGCTGTCGCACTCCCTCTCTCCCTACGCCGAGGAAAGCACCATGCTCAAACTCACCGC
       D  Q  I  P  G  G  G  F  Q  F  E  L  S  H  S  L  S  P  Y  A  E  E  S  T  M  L  K  L  T  A  186
721  TGAGGCCATTATTAACTTCTCCATCTTCAGGATGACCAAGACATTTTATCTTCGAGACATTGTTCAACCCGACAGTCCCCAGATTAGCAC
       E  A  I  I  N  F  S  I  F  R  M  T  K  T  F  Y  L  R  D  I  V  Q  P  D  S  P  Q  I  S  T  216
811  GTGTCAGGAGATGGAGCAGAACCTGAAAGTGACCATCGATCCTCCATCCAGCTGGTCCACCCCTGAGAGTTTCTTCTGTCTGGAGCACGA
       C  Q  E  M  E  Q  N  L  K  V  T  I  D  P  P  S  S  W  S  T  P  E  S  F  F  C  L  E  H  E  246
901  GATTGAATACGTGTTCAAAGATGATGGGAAGACTGGACGCTCTTTCTCTTCCCTGATACCGAAGAGCATCAGTAAGCTGAGGGTCCGCTC
       I  E  Y  V  F  K  D  D  G  K  T  G  R  S  F  S  S  L  I  P  K  S  I  S  K  L  R  V  R  S  276
991  CAGAGACTCGCTGGTGCTCTCAACCTGGAGCAATTGGACTCCTTGGAAAATGTGAggtcgcgggaagagaacttgtgcaaatgcagaaac
       R  D  S  L  V  L  S  T  W  S  N  W  T  P  W  K  M  *                                    293
1081 acagtaaaatattgctgtccagagttgccacctgcattgttggaacgctgcaagaagaagaagaagatgaagaagaagaaaaagaac
1171 aagacatcttaaaaacatgttgaataaaaaggtacattgctgctgggatcattctgtcgcacaaacacaccacagttagtggagaataat
1261 gaacaaataattgcttacgtgtgtgagtatgaagcaaataaagtgttgtatgttattgc
```

Fig. 1. cDNA and deduced amino acid sequences of olive flounder *IL-12*. (A) The sequences of the *IL-12p35* subunit and (B) *IL-12p40* subunit. The sequence of the coding region is capitalized with the deduced amino acids. The start codon (ATG) and stop codons (TGA, TAA) are indicated in bold. Polyadenylation signals (AATAAA) are underlined. The putative signal peptide is shaded in grey.

agarose beads (Qiagen, USA) with a minor modification of the manufacturer's protocol. Briefly, the fresh-overnight recombinant *E. coli* BL-21 culture (1% v/v) was inoculated into 1 L of LB media and incubated at 37 °C with rotation (150 rpm) until it reached an OD_{600} of 0.6. Following induction with 400 μM IPTG, the cultivation continued for 4 more hours. The bacterial pellet was collected by centrifugation at 5000 g for 10 min at 4 °C and stored at −80 °C until use. The pellet was lysed by adding 100 ml 8 M urea, 100 mM NaH_2PO_4, and 10 mM Tris-Cl pH 8.0 with 3000 units Benzonase followed by a 1-h incubation at 25 °C until the lysate became clear. A purification column was prepared with

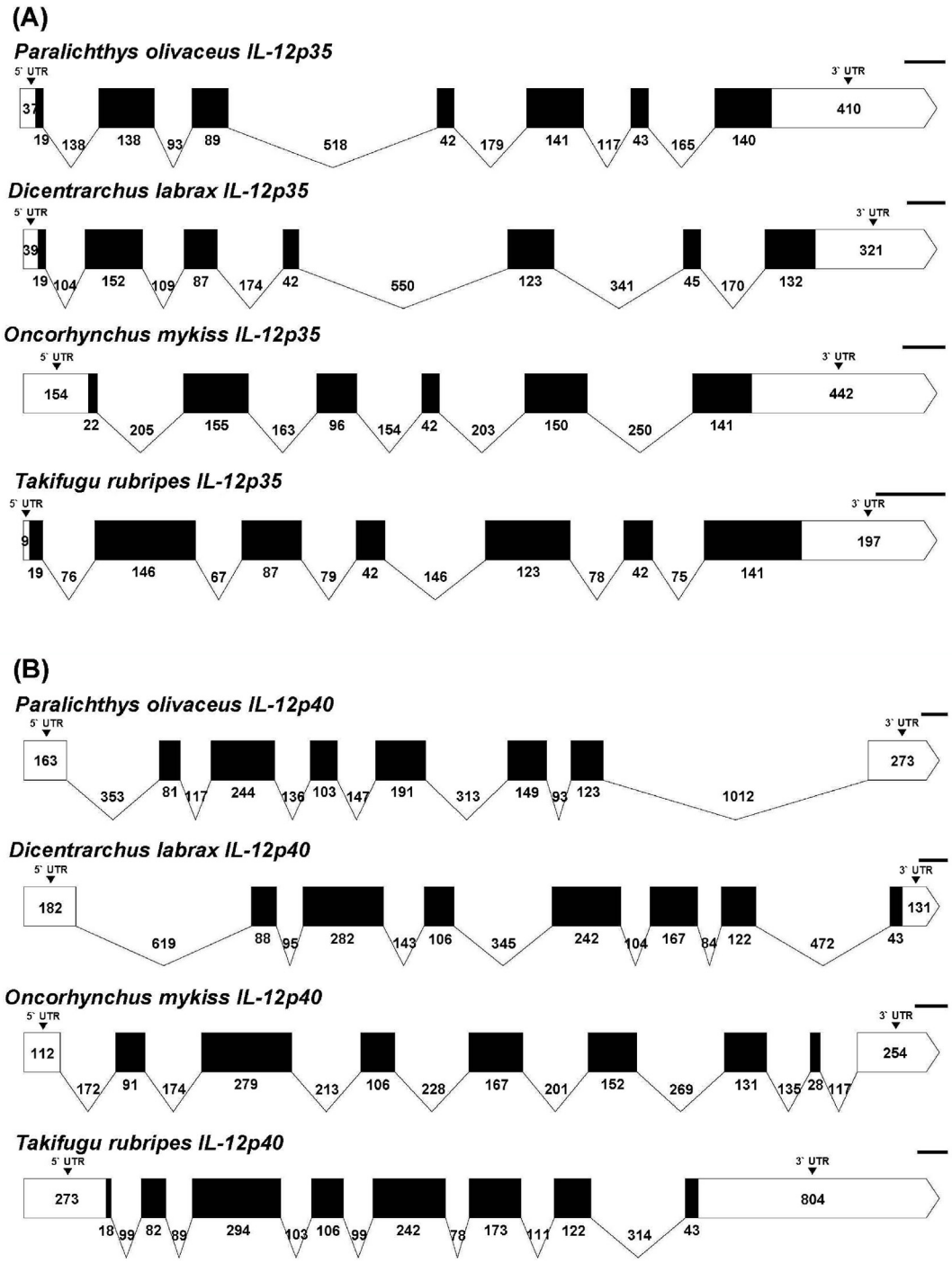

Fig. 2. Diagrammatic comparison of IL-12 gene structures. The gene structures of *IL-12p35* (A) and *IL-12p40* (B) of olive flounder are shown alongside those of European bass, rainbow trout, and Japanese puffer. Exons are represented by black boxes and length is shown below the box. Intron length in base pairs is shown on top of the line.

3 ml of Ni-NTA slurry and equilibrated with 10 ml of 8 M urea. Following centrifugation of the lysate for 15 min at 4000 rpm at 4 °C, the supernatant was slowly loaded onto the column, and the column was washed with 200 ml (approx. 20 column volume) of washing buffer containing 8 M urea, 100 mM, NaH_2PO_4, and 10 mM Tris-Cl, pH 6.3. Then, the rIL-12 protein was eluted with 5 ml of elution buffer containing 8 M urea, 100 mM NaH_2PO_4, and 10 mM Tris-HCl, pH 5.9. The eluted rIL-12 protein was further refolded via serial diafiltration using 30 kDa nominal molecular weight limit (NMWL) Amicon® Ultra-15 centrifuge tubes. Five ml of rIL-12 eluate was slowly diluted with 10 ml of 6 M urea, 100 mM NaH2PO4, and 10 mM Tris-HCl, pH 5.9 and was diafiltrated by centrifugation in the Amicon® Ultra-15 tube for 15 min at 4000 rpm. The residue was slowly diluted again with 10 ml of 4 M urea with the same salt concentration. The dilution and diafiltration procedure was repeated with 2, 1, 0.5, 0.25 M urea and finally 3 times with PBS to remove remaining urea completely. The protein that was still insoluble was discarded. The soluble rIL-12 was confirmed by PAGE-Coomassie blue staining, quantified by bicinchoninic acid assay (BCA), and stored at 4 °C until use.

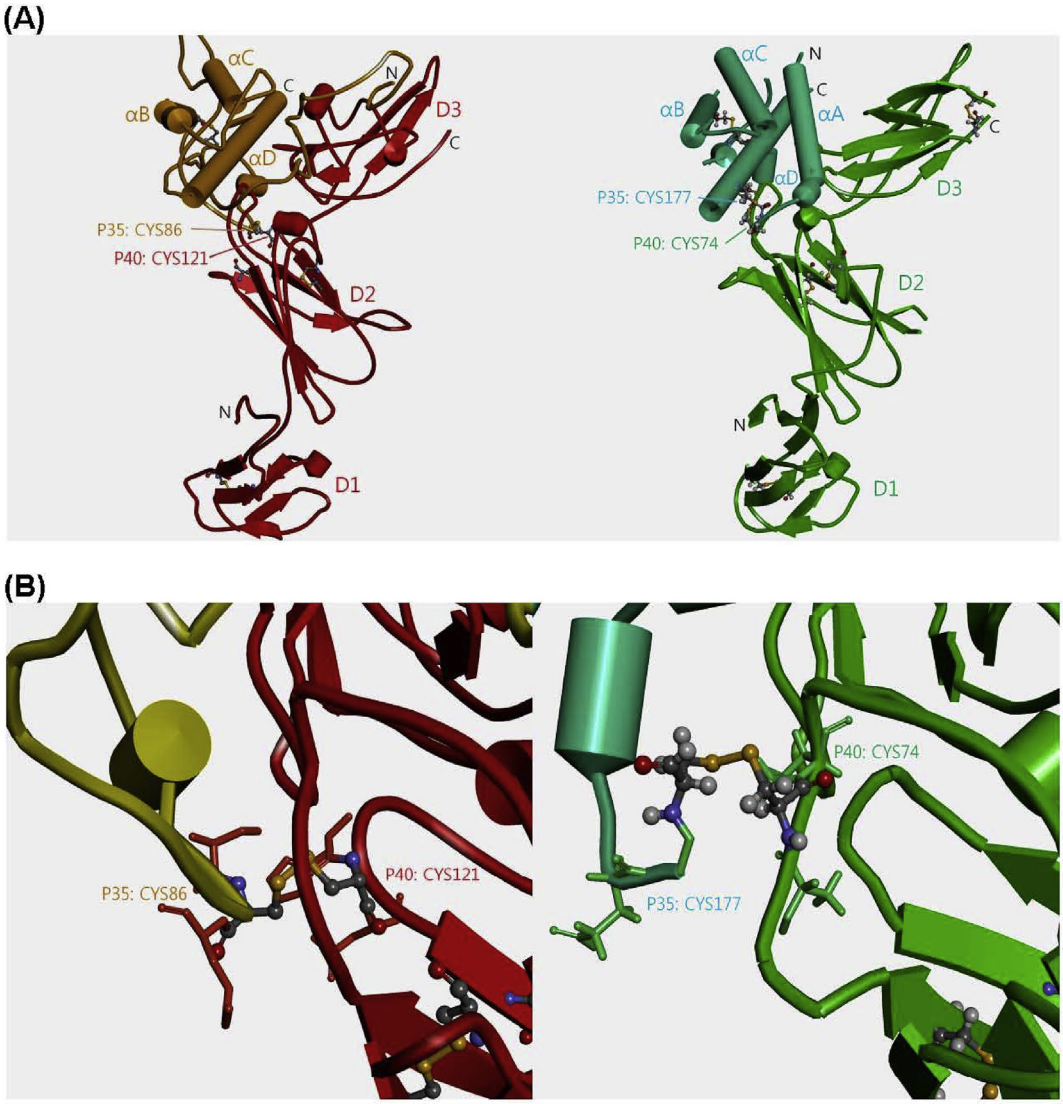

Fig. 3. Structural model analysis of olive flounder IL-12. (A) The left panel indicates the structural model of flounder IL-12 (red) while the right panel depicts the human IL-12 structure (green). Protein backbones and secondary structures are presented in schematic form while the cysteine-cysteine disulfide bond is shown in ball and stick form. The N and C termini of IL-12p35 and p40 are indicated in black. The immunoglobulin domains of IL-12p40 are shown as D1, D2, and D3, while the α-helix of p35 is shown as αA, αB, αC, and αD. Cysteine inter-chain disulfide bonds are indicated in orange, labeled with specific numbers of amino acids. In human, the cysteines responsible for connecting p35 and p40 subunits are Cys177 of p35 and Cys74 of p40. The comparable cysteine residues of olive flounder IL-12 that were predicted on the basis of the human IL-12 structure are Cys86 of p35 and Cys121 of p40. (B) The expanded graphical display of the p35 and p40 inter-chain disulfide bonds are shown: the olive flounder IL-12 structure is shown in the left panel (red) while the human IL-12 structure is shown in the right panel (green). (For interpretation of the references to colour in this figure legend, the reader is referred to the Web version of this article.)

2.8. Bioactivity of the single-chain olive flounder rIL-12

2.8.1. Preparation of olive flounder PBMC and functional test of olive flounder rIL-12

Blood samples were collected from the caudal vein of olive flounder in BD Vacutainer® blood collection tubes containing sodium citrate (BD, UK). Red blood cells (RBC) were eliminated by RBC Lysis buffer (Invitrogen, USA) according to the manufacturer's manual. PBMC (peripheral blood mononuclear cells) were then suspended in L-15 media (Fisher Scientific, USA) supplemented with 10% fetal bovine serum (Fisher Scientific, Australia), 100 units/ml penicillin, and 100 μg/ml streptomycin (Fisher Scientific, USA). Various concentrations of the olive flounder rIL-12 (1000 ng/mL, 100 ng/mL, or none) were added to the cells seeded in a 12-well plate (5×10^7 cells/well) and further incubated overnight at 25 °C. Following the addition of 600 μl of the RLT lysis buffer (Qiagen, Netherlands) with 40 mM DTT (Dithiothreitol), the cells were kept at −20 °C until use.

2.8.2. RNA extraction and cDNA synthesis

RNA was extracted from the rIL-12-treated olive flounder PBMC using TaKaRa MiniBEST Universal RNA Extraction Kit (Takara, Kusatsu, Japan) according to the manufacturer's instruction. Qualification and Quantification of RNA were determined by a SPECTROstar Nano (BMG LABTECH, Ortenberg, Germany). cDNA was synthesized using 400 ng of each RNA sample using SuperScript® III First-Strand Synthesis System for RT-PCR (Invitrogen, Carlsbad, USA) according to the manufacturer's direction.

2.9. Neutralization test of endogenous olive flounder IL-12 by anti-olive flounder rIL-12 antibody

2.9.1. Production of anti-olive flounder rIL-12 mouse antibody

Six-week-old ICR female mice were maintained on a 12-h dark/12-h light cycle. Three ICR mice were immunized three times (days 1, 5, and 15) with 100 μg of rIL-12 mixed with Freud's complete adjuvant (Santa

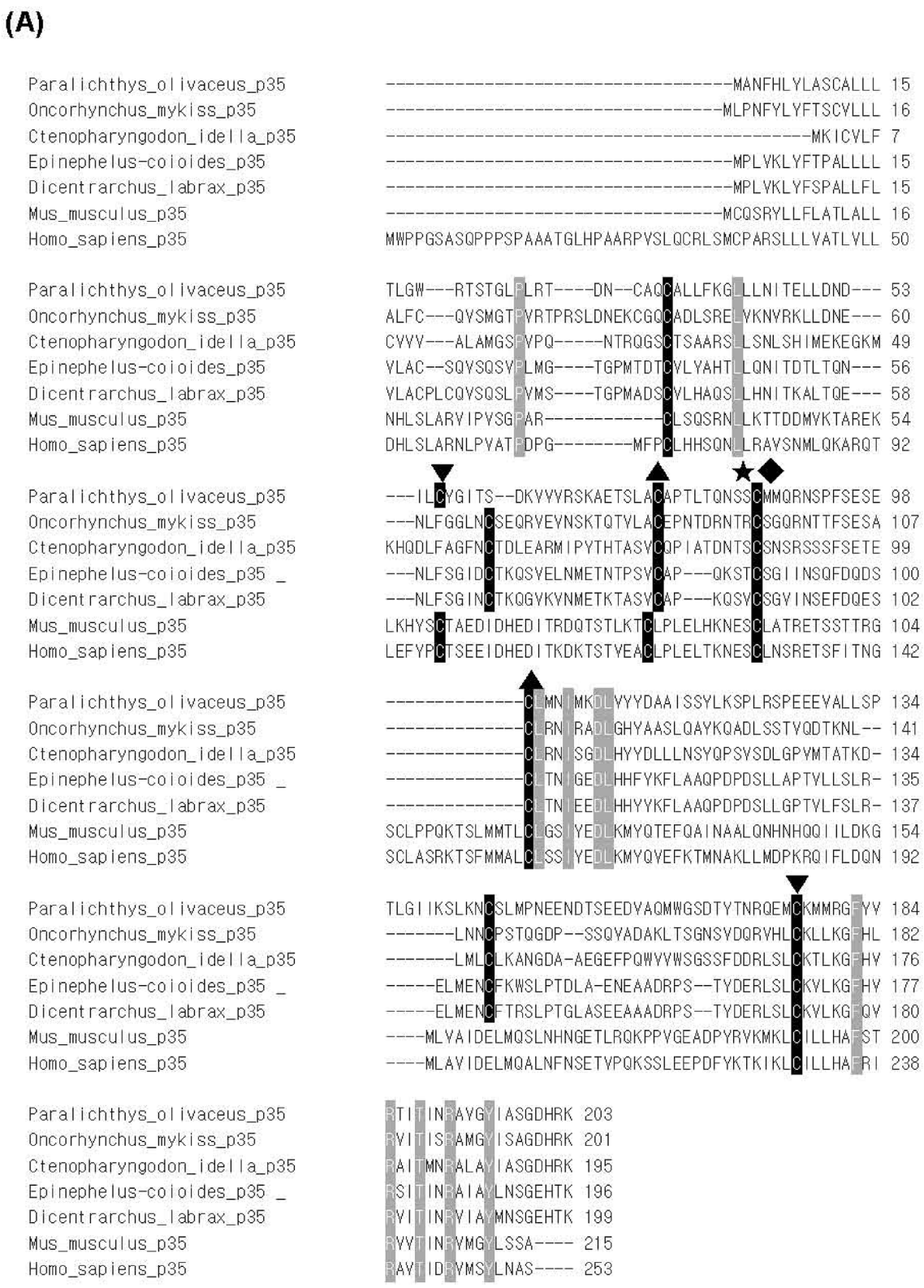

Fig. 4. Multiple alignments of olive flounder IL-12 amino acid sequences. Amino acid sequences of the IL-12p35 (A) and IL-12p40 subunits (B) were aligned in comparison to those of 4 teleost fish, mouse, and human. Identical protein residues are shown in grey blocks with white letters with cysteine residues in black blocks with white letters. Predicted cysteine-cysteine bonds are marked with (†, ‡, ▼, ▲) on top of the sequence. The sites of the inter-chain disulfide bond identified for human p35 and p40 are indicated with (◆), whereas the sites predicted for olive flounder IL-12 subunits are shown with (★).

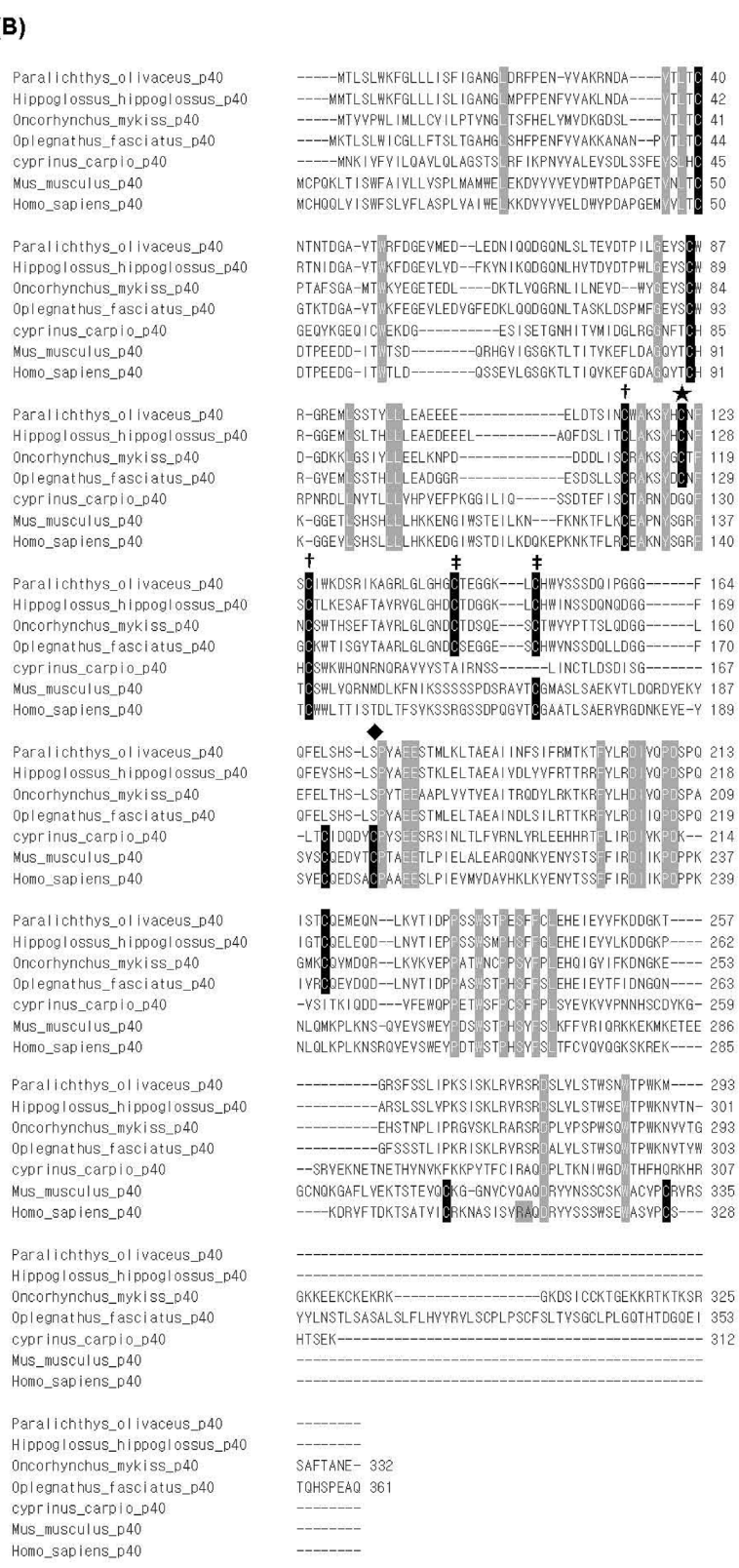

Fig. 4. (*continued*)

Cruz Biotechnology, Dallas, USA). Three days after the third immunization (day 18), mice were anesthetized for blood collection by cardiac puncture leading to euthanasia. Serum was collected from 500 μl blood diluted in 1 ml PBS following centrifugation for 10 min at 13,000 rpm at 4 °C. After titration, the anti-olive flounder rIL-12 mouse antibody was stored at −80 °C until use.

2.9.2. Neutralization of natural olive flounder IL-12 by anti-olive flounder rIL-12 mouse antibody

Olive flounder PBMC in a 24-well plate (5×10^7 cells/well) were treated with LPS (25 μg/mL) to induce natural IL-12 production. Following the addition of *anti*-rIL-12 mouse antibody (1:400 dilution), the cells were incubated for 6 h at 25 °C. The olive flounder PBMC

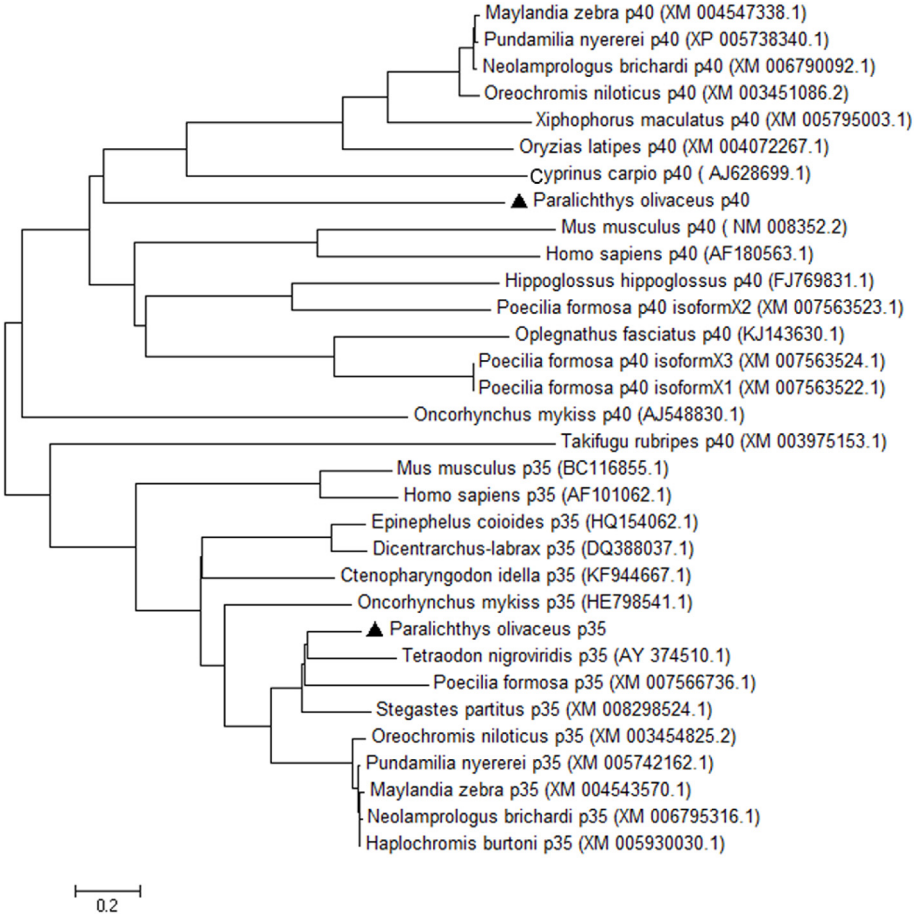

Fig. 5. The phylogenetic tree of IL-12. The IL-12 phylogenetic tree was constructed using the neighbor-joining method using MEGA 6 with 1000 times of bootstrapping. The accession numbers of the compared genes are shown in parentheses.

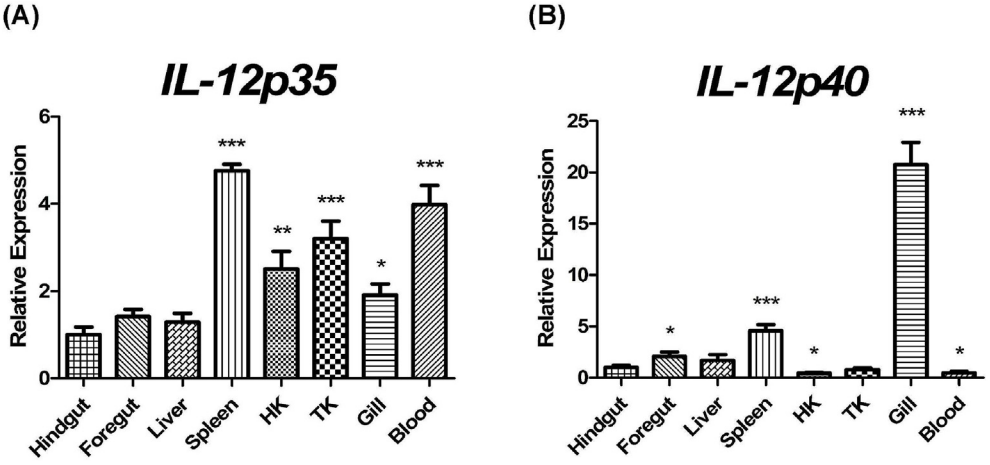

Fig. 6. *IL-12* expression profiles in olive flounder tissues in the natural state without stimulation. Relative expression of *IL-12* subunit genes was assessed in various tissues of olive flounder in a native state without stimulation. The expression level of *β-actin* was used as an internal control for normalization. HK stands for head kidney and Tk, trunk kidney. The mean value is shown with the ± S.E.M difference in mRNA expression level compared to the control group. *P < 0.05; **P < 0.01; ***P < 0.001.

treated with the olive flounder rIL-12 (200 ng/mL) along with the antibody was also included as a control. RNA was extracted from the cells, and the expression of cytokine genes was analyzed using the qRT-PCR method.

2.10. Statistical analysis

Statistical significance was evaluated using an unpaired two-tailed student's t-test and one-way analysis of variance (ANOVA) using Graph Pad Prism 5 software. Significant differences are presented as follows: *P < 0.05; **P < 0.01; ***P < 0.001.

3. Results

3.1. cDNA sequence of olive flounder IL-12

The full-length cDNA sequences of *IL-12p35* and *IL-12p40* subunits were identified. The size of the *IL-12p35* cDNA was 1059 base pairs (bp), within which 612 bp of open reading frame (ORF) was included (Fig. 1A). The *IL-12p35* cDNA contained a 37 bp-5'untranslated region (UTR) and a more extended 3′UTR (410 bp) with the polyadenylation (poly-A) signal at the 14-bp upstream of the poly-A tail. The total length of the *IL-12p40* cDNA was 1319-bp including the 882 bp-ORF (Fig. 1B).

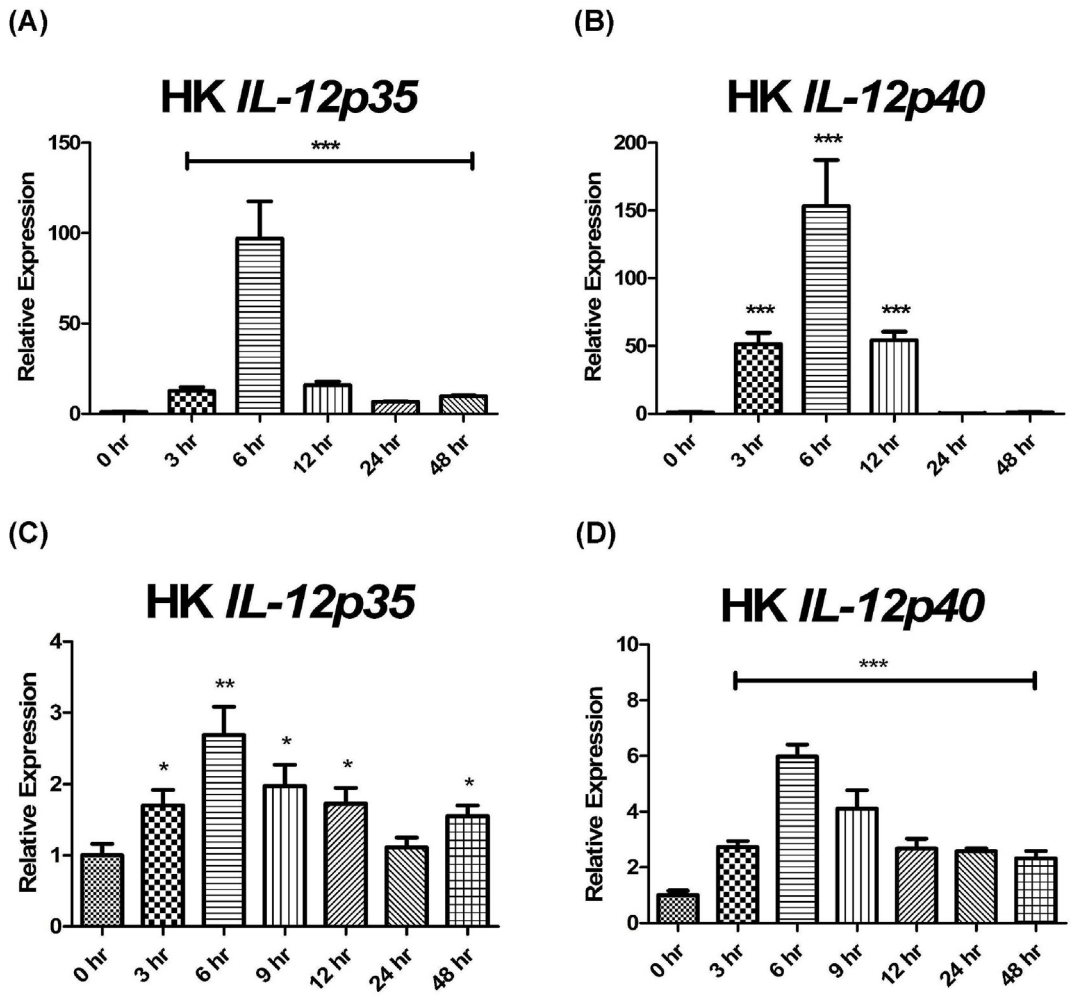

Fig. 7. Time-dependent expression profiles of olive flounder *IL-12* in the head kidney after stimulation. Olive flounder were exposed to either LPS *i.v.* (A, B) or *E. tarda* infection (C, D), and the time-course of IL-12 expression in the head kidney was analyzed. The mean values are shown with the ± S.E.M difference in mRNA expression level compared to the control group. *P < 0.05; **P < 0.01; ***P < 0.001.

The lengths of 5′UTR and 3′UTR were 163 bp and 274 bp, respectively. The *IL-12p40* cDNA included two poly-A signals; one was located at the 1297 bp position and the other at the 1193 by position. Indeed, two different sizes of the *IL-12p4*0 RNA were produced from the same gene although the larger one was expressed at higher levels (data not shown).

3.2. Gene structure of olive flounder IL-12

The olive flounder *IL-12p35* gene is comprised of seven exons and six introns while the *IL-12p40* gene consists of six exons and seven introns (Fig. 2). The exon numbers of both subunits of the olive flounder *IL-12* are the same as those of the human *IL-12* gene. However, the olive flounder *IL-12* gene contains one fewer exon than the rainbow trout in both subunit genes. All exon-intron junctions of the olive flounder *IL-12* followed the GT/AG rule, except the second and the last introns of both *IL-12p35* and *IL-12p4*0 that utilized the minor splicing sites, AT/AC.

3.3. Structural analysis of olive flounder

As shown in Fig. 3A, the homology model of the olive flounder IL-12p35 protein structure was similar to that of the known human IL-12p35 structure; the α-helixes and β sheets at the B, C, and D regions corresponded to each other correctly. The olive flounder IL-12p40 protein structure is composed of three immunoglobulin domains (D1, D2, D3), which also correctly correspond to their human counterparts. Furthermore, the domain containing the disulfide bond that connects the two subunits of IL-12 was very similar structurally between the olive flounder and human IL-12 (Fig. 3B). These data allowed the prediction of cysteine residues responsible for the disulfide bonding between IL-12p35 and IL-12p40 for the formation of the functional olive flounder IL-12 protein: Cys86 of p35 and Cys121 of p40. The DOPE score of the flounder IL-12 structural model (−41758.7) was close to that of the human IL-12 (−45310.6), indicating that the flounder IL-12 model is likely to fold similarly to human IL-12.

3.4. Multiple sequence alignment of IL-12 gene

The alignment of the IL-12 amino acid sequences of fish, mouse, and human showed similar patterns in many conserved regions (Fig. 4). The cysteine residues in olive flounder IL-12p35 that might be responsible for the disulfide linkage between IL-12p35 and IL-12p40 subunits were conserved among fish and even mammals, including humans (Figs. 3 and 4). In contrast, the positions of the cysteine responsible for the disulfide bonding showed some variation. The cysteine position in olive flounder IL-12p40 was highly conserved among those of Atlantic halibut, striped beakfish, and rainbow trout; however, the cysteine site was different from that in common carp, mammal, and human (all of which share the same position of the cysteine residue).

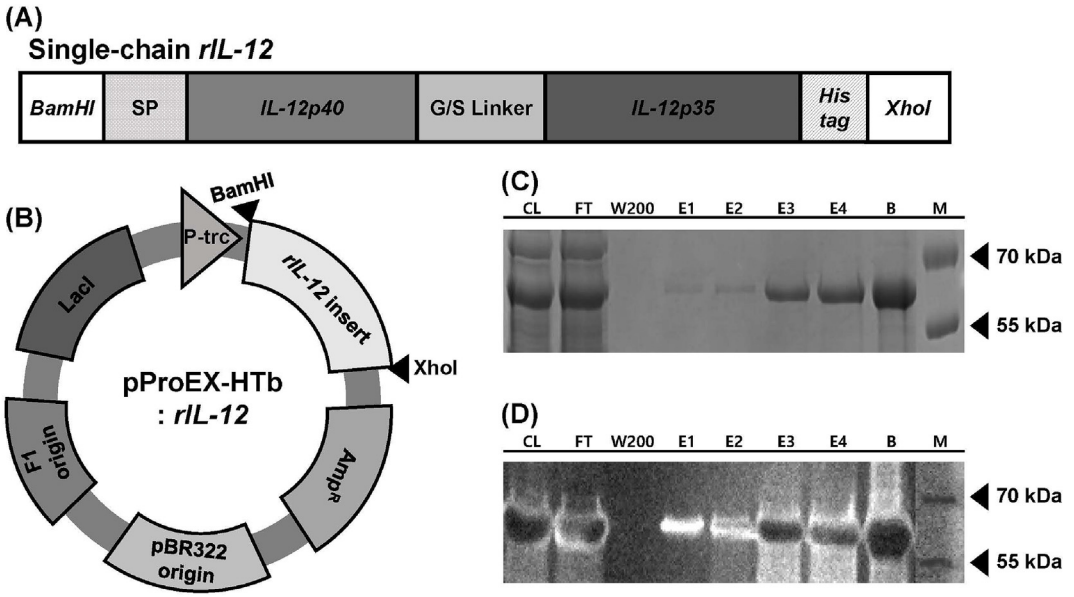

Fig. 8. Construction of functional, recombinant olive flounder IL-12. Biologically active recombinant IL-12 was generated by connecting the *IL-12p40* and *IL-12p35* subunit cDNAs with a G/C linker. (A) Schematic diagram of the recombinant *IL-12* (*rIL-12*) cDNA in which the cDNAs of the two subunit genes were fused. Abbreviation: SP, signal peptide. (B) Illustration of the single-chain rIL-12 cDNA inserted into an expression vector, pProEX-HTb. Abbreviations: P-trc, trc promoter; Amp^R, ampicillin resistance gene; LacI, lactose operon repressor. (C) Protein purification profiles of rIL-12: lane 1, clear lysate; lane 2, flow through; lane 3, wash at 200 mL fraction; lane 4–7, successive eluants 1 ml each; lane 8, beads; lane 9, size marker. (D) Western blot analysis of the rIL-12 purification profiles shown in (C).

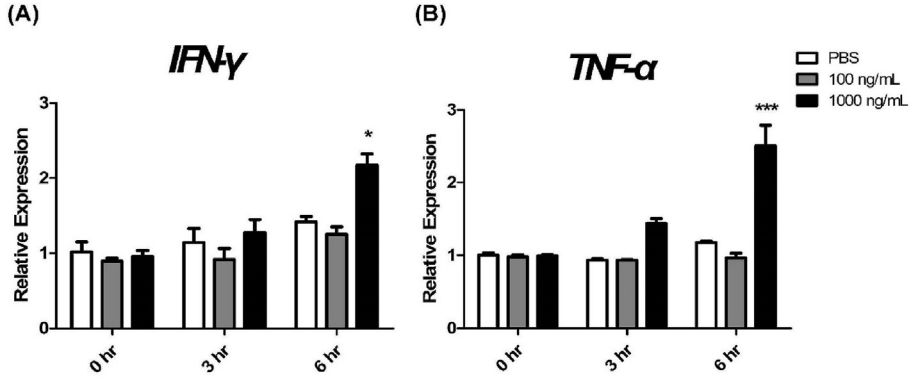

Fig. 9. Production of cytokines by olive flounder PBMC induced by the rIL-12. Biological activities of the rIL-12 were assessed by the capability to induce production of pro-inflammatory cytokines. (A) Time and dose-dependent IFN-γ production in olive flounder PBMC treated with rIL-12. (B) Expression of TNF-α in olive flounder PBMC induced with rIL-12. The mean value was shown with the ± S.E.M difference in mRNA expression level compared to the PBS-treated control group. *P < 0.05; **P < 0.01; ***P < 0.001.

3.5. Phylogenetic tree analysis

The phylogenetic tree of IL-12 constructed by the neighbor-joining method resulted in two clusters: IL-12p40 and IL-12p35 (Fig. 5). Olive flounder IL-12p40 was close phylogenetically to common carp but was remote from that of rainbow trout. Olive flounder IL12-p35 was strictly related to green-spotted puffer, but less related to *H. burtoni*.

3.6. IL-12 gene expression in olive flounder tissues

The subunit genes of olive flounder *IL-12* were differentially expressed in the same tissue regardless of the flounder's condition (Fig. 6A and B). *IL-12p35* was expressed at the highest level in spleen, trunk kidney, and blood, but was also expressed at lower levels in the gut and liver. *IL-12p40* was expressed at the highest levels in the blood and gill, but at lower levels in the gut, liver, and kidney. However, when olive flounder were stimulated with LPS (Fig. 7A and B) or pathogen infection (Fig. 7C and D), the expression patterns of *IL-12* subunit genes became similar to each other. In head kidney tissue of LPS-injected olive flounder, both of the subunit genes gradually increased expression and reached maximum levels at 6 h post-treatment (Fig. 7A and B). Then, the level of expression diminished and returned to the basal level after an additional 48 h. However, the rate of decrease in expression was faster for *IL-12p35* as compared to *IL-12p40*. These patterns of time-dependent *IL-12* expression were similar when olive flounder was infected with a pathogen, *E. tarda* (Fig. 7C and D); maximum *IL-12* expression reached at 6 h post-infection, after which expression gradually declined. However, the *IL-12p40* gene took longer to return to basal level expression than *IL-12-p35,* although the difference was not significant.

3.7. Generation of single-chain olive flounder rIL-12 and functional analyses of the rIL-12

Functional olive flounder *IL-12* was constructed by connecting the cDNAs of the *IL-12p35* and *IL-12p40* subunit genes with a G/S linker (Fig. 8A). Single chain IL-12 was purified after expression via a recombinant vector, pProEX-HTb, into which the fused *IL-12* was cloned at the BamHI and XhoI sites (Fig. 8B). The size of the purified rIL-12 was approximately 60 kDa, as confirmed by Coomassie blue staining (Fig. 8C) and western blot analysis (Fig. 8D).

The biological activity of the single-chain olive flounder rIL-12 was confirmed by testing the ability of olive flounder PBMC to produce cytokines after treatment with the rIL-12 (1 μg/ml). The rIL-12-treated

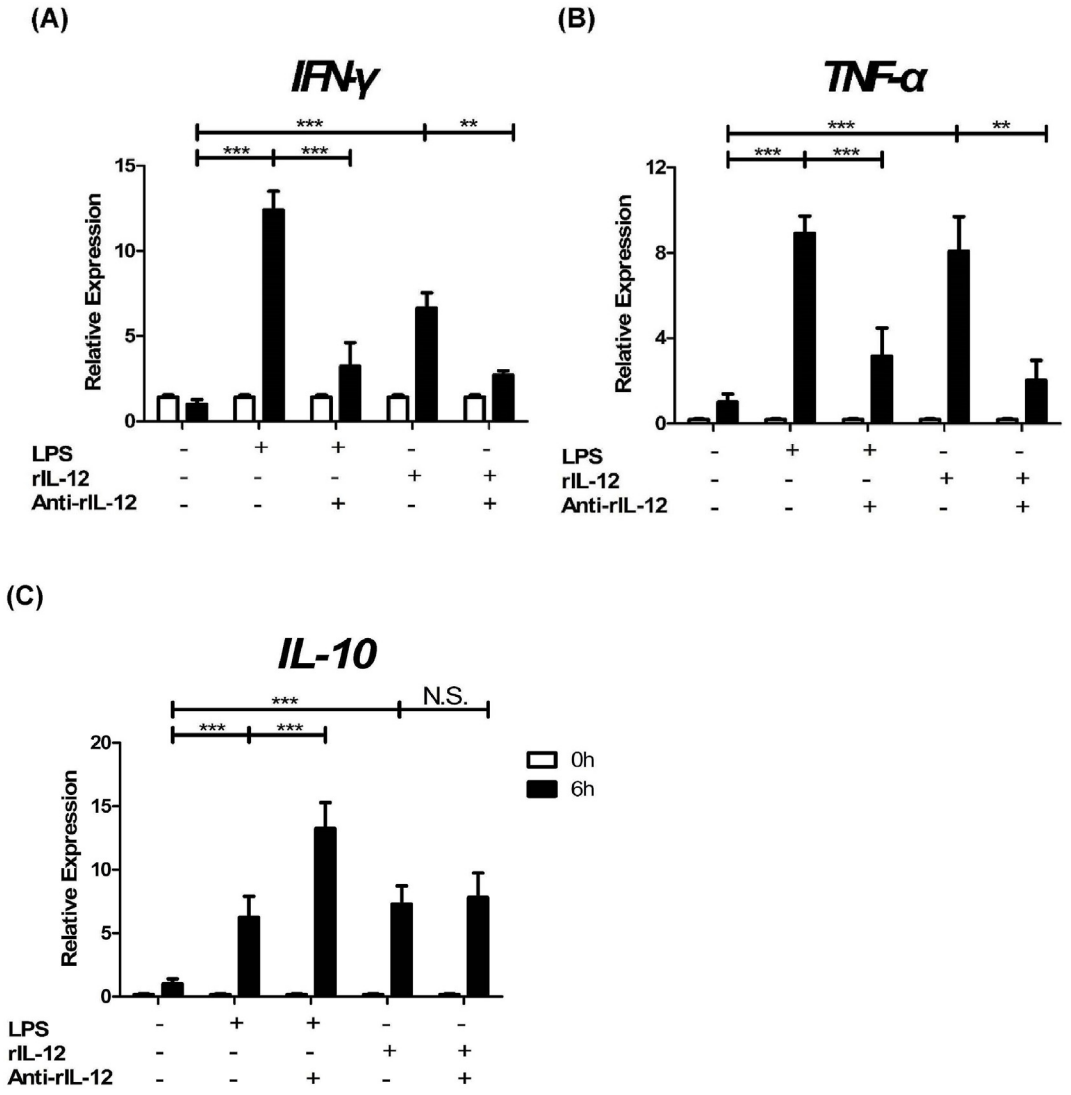

Fig. 10. Neutralization of intrinsic olive flounder IL-12 by mouse anti-olive flounder rIL-12 antibody. Functional activities of the single-chain rIL-12 were further evaluated by assessing the neutralizing activity of the antibody against endogenous IL-12. The status of IL-12 neutralization of the antibody was appraised by monitoring the inhibition of expression of cytokines known to be induced by IL-12. (A) The relative expression level of *IFN-γ* in olive flounder PBMC. (B) The relative expression level of *TNF-α* in olive flounder PBMC. (C) The relative expression level of *TNF-α* in olive flounder PBMC. The relative expression level of *IL-10* in olive flounder PBMC. The mean value is shown with the ± S.E.M difference in mRNA expression level compared to the PBS-treated control group. $P < 0.05$; $^{**}P < 0.01$; $^{***}P < 0.001$.

cells significantly increased the production of IFN-γ at 6 h post-treatment (Fig. 9A). TNF-α was also produced by PBMC treated with the single-chain rIL-12 in a similar manner (Fig. 9B). The function of single-chain rIL-12 was further assessed with a neutralizing assay utilizing an anti-olive flounder rIL-12 mouse antibody. Olive flounder PBMC treated with LPS, a well-known stimulator of IL-12 production, or with rIL-12; both groups significantly produced *IFN-γ,* which is known to be induced by IL-12 (Fig. 10A). When the rIL-12-specific neutralizing antibody was added to the olive flounder PBMC treated with LPS or rIL-12, both of the groups exhibited significantly reduced *IFN-γ* expression. These data indicate the rIL-12-specific antibody neutralized the natural IL-12 induced by LPS. Similar results were obtained in a similar experiment measuring TNF-α production, which is also known to be stimulated by IL-12 (Fig. 10B); PBMC stimulated with LPS, or rIL-12 expressed significantly higher levels of *TNF-α* while expression was markedly inhibited after treatment with the rIL-12-specific neutralizing antibody. However, IL-10, a primary antagonist of IFN-γ, was produced after treatment with the IL-12 neutralizing antibody (Fig. 10C).

4. Discussion

The data presented here demonstrate: (i) the nucleotide sequence and gene structure of olive flounder *IL-12* subunits, *IL-12p35* and *IL-12p40*; (ii) the tissue distribution of the *IL-12* gene expression; (iii) identification of the cysteine residues responsible for the disulfide bond between IL-12 subunits as determined through structural modeling; and (iv) the function of olive flounder IL-12 via experiments utilizing a single-chain olive flounder rIL-12 and neutralizing rIL-12-specific mouse antibody. The reported *IL-12p35* and *IL-12p40* gene structures of teleost vary significantly; the sizes and numbers of exons and introns are different even among the phylogenetically close fish species. Surprisingly, this variation exists even within salmonids, although it is not as dramatic [30]. The gene structure of olive flounder *IL-12* was also dissimilar to those of rainbow trout and human. Although *IL-12p35* mRNA contained only one polyadenylation signal at the 3' end, there were two polyadenylation signals present in *IL-12p40* mRNA. Indeed, *IL-12p40* expressed two types of mRNA: a longer *IL-12p40* mRNA was expressed at higher levels than the shorter one under both intrinsic and

induced states (data not shown). Although the IL-12p40 subunit of IL-12 is utilized by both IL-12 and IL-23, the utilization of these mRNA molecules may be different. However, the properties of the IL-12p40 mRNA subtypes need to be further explored.

The structural models of olive flounder IL-12 subunits were very similar to those of the human counterpart; The positions of the α-helix and β-sheet immunoglobulin domains corresponded precisely. Furthermore, the region around the disulfide bond that interconnects the two subunits of human IL-12 was structurally the same as that of flounder IL-12. Therefore, we propose that Cys86 of IL-12p35 and Cys121 of IL-12p40 may be responsible for the disulfide bond that connects subunit proteins of olive flounder IL-12; however, this needs to be further confirmed by X-ray crystallography, NMR spectroscopy, and dual polarization interferometry. When the sequences around this intermolecular disulfide bond were compared, the cysteine position at the IL-12p35 was conserved among all the species tested, including various fish, mouse, and human. However, the positions of the counterpart cysteine residue at the IL-12p40 exhibited some variation among species. This positional variation of the cysteine residue may be due to subtle variations in the region between the D2 and D3 domains of the IL-12 structure.

Olive flounder lymphoid organs such as the spleen and the head kidney constitutively expressed *IL-12* at low levels under uninfected conditions. However, the expression level of *IL-12p40* was relatively high compared to that of *IL-12p35* in contrast to mammals which express *IL-12p35* at higher levels [2,7]. Although the underlying mechanism is not understood at present, fish and mammals may differ in the gene regulation of *IL-12p40* and the utilization of its product during the process of IL-23 synthesis, which shares the IL-12p40 subunit with IL-12. However, when the fish were infected by *E. tarda* or stimulated by LPS, the head kidney expressed both of the *IL-12* subunit genes at comparable levels. The head kidney of bony fish is known to be the organ of hematopoiesis in which various kinds of immune cells are produced from pluripotent stem cells [31,32]. In addition, the subunit genes showed similar time-dependent expression patterns as well: gene expression increased and reached maximum levels at 6 h post-treatment and gradually decreased thereafter.

IL-12 stimulates the production of IFN-γ and TNF-α from T cells and natural killer (NK) cells and mediates the enhancement of cytotoxic activity in NK cells and $CD8^+$ T cells [39,40]. IL-10 controls the production of these essential pro-inflammatory cytokines by suppressing IL-12 activity; conversely, IFN-γ inhibits IL-10 production [34,35]. IFN-γ and IL-10 antagonize each other's production and function, which results in a balance between pro-inflammatory and anti-inflammatory status [36]. When olive flounder PBMC were treated with single chain rIL-12, the cells exhibited significantly higher levels of *IFN-γ* and *TNF-α* gene expression like LPS, a well-known inducer of these pro-inflammatory cytokines. However, the LPS-treated flounder PBMC exhibited significantly reduced expression of *IFN-γ* and *TNF-α* genes when the *anti*-rIL-12-specific antibody was added to the culture medium; *IL-10* expression was significantly increased instead. These data confirmed the accurate identification of olive flounder IL-12 subunit genes and the functional capacity of olive flounder IL-12.

In conclusion, the present article presents the first identification of the olive flounder *IL-12* gene. The supporting evidence includes the structure of the olive flounder *IL-12* gene and the function of the IL-12 protein produced. IL-12 function was confirmed by generating single chain rIL-12 and an *anti*-rIL-12-specific mouse antibody. Functional rIL-12 and its specific antibody may be useful as reagents for studying the molecular mechanisms involved in immune regulation in olive flounder. In addition, the rIL-12 molecule may also be used as an adjuvant for fish vaccines including those for olive flounder.

Acknowledgments

This study was supported by the National Research Foundation of the Republic of Korea (NRF-2015R1D1A1A01056959), and also by the Basic Research Project (19-3214) of the Korea Institute of Geoscience and Mineral Resources (KIGAM) funded by the Ministry of Science and ICT.

References

[1] E. Macatonia Steven, et al., Dendritic cells produce IL-12 and direct the development of Th1 cells from naive CD4+ T cells, J. Immunol. 154 (10) (1995) 5071–5079.
[2] Xiaojing Ma, et al., The interleukin 12 p40 gene promoter is primed by interferon gamma in monocytic cells, J. Exp. Med. 183 (1) (1996) 147–157.
[3] Trinchieri Giorgio, Interleukin-12 and the regulation of innate resistance and adaptive immunity, Nat. Rev. Immunol. 3 (2) (2003) 133–146.
[4] T. Watford Wendy, et al., The biology of IL-12: coordinating innate and adaptive immune responses, Cytokine Growth Factor Rev. 14 (5) (2003) 361–368.
[5] Mark P. Hayes, Jinhai Wang, Norcross Michael A, Regulation of interleukin-12 expression in human monocytes: selective priming by interferon-gamma of lipopolysaccharide-inducible p35 and p40 genes, Blood 86 (2) (1995) 646–650.
[6] Chyi-Song Hsieh, et al., Development of TH1 CD4+ T cells through IL-12 produced by Listeria-induced macrophages, Science 260 (5107) (1993) 547–549.
[7] D'Andrea Annalisa, et al., Production of natural killer cell stimulatory factor (interleukin 12) by peripheral blood mononuclear cells, J. Exp. Med. 176 (5) (1992) 1387–1398.
[8] Michiko Kobayashi, et al., Identification and purification of natural killer cell stimulatory factor (NKSF), a cytokine with multiple biologic effects on human lymphocytes, J. Exp. Med. 170 (3) (1989) 827–845.
[9] S. Stern Alvin, et al., Purification to homogeneity and partial characterization of cytotoxic lymphocyte maturation factor from human B-lymphoblastoid cells, Proc. Natl. Acad. Sci. Unit. States Am. 87 (17) (1990) 6808–6812.
[10] A. Cassatella Marco, et al., Interleukin-12 production by human polymorphonuclear leukocytes, Eur. J. Immunol. 25 (1) (1995) 1–5.
[11] Trinchieri Giorgio, Interleukin-12: a cytokine produced by antigen-presenting cells with immunoregulatory functions in the generation of T-helper cells type 1 and cytotoxic lymphocytes, Blood 84 (12) (1994) 4008–4027.
[12] Manetti Roberto, et al., Natural killer cell stimulatory factor (interleukin 12 [IL-12]) induces T helper type 1 (Th1)-specific immune responses and inhibits the development of IL-4-producing Th cells, J. Exp. Med. 177 (4) (1993) 1199–1204.
[13] Trinchieri Giorgio, Interleukin-12: a pro-inflammatory cytokine with immunoregulatory functions that bridge innate resistance and antigen-specific adaptive immunity, Annu. Rev. Immunol. 13 (1) (1995) 251–276.
[14] F. Wolf Stanley, et al., Cloning of cDNA for natural killer cell stimulatory factor, a heterodimeric cytokine with multiple biologic effects on T and natural killer cells, J. Immunol. 146 (9) (1991) 3074–3081.
[15] K. Gately Maurice, et al., Regulation of human lymphocyte proliferation by a heterodimeric cytokine, IL-12 (cytotoxic lymphocyte maturation factor), J. Immunol. 147 (3) (1991) 874–882.
[16] Jalah Rashmi, et al., The p40 subunit of interleukin (IL)-12 promotes stabilization and export of the p35 subunit implications for improved IL-12 cytokine production, J. Biol. Chem. 288 (9) (2013) 6763–6776.
[17] Ping Ling, et al., Human IL-12 p40 homodimer binds to the IL-12 receptor but does not mediate biologic activity, J. Immunol. 154 (1) (1995) 116–127.
[18] Yasutoshi Yoshiura, et al., Identification and characterization of *Fugu* orthologues of mammalian interleukin-12 subunits, Immunogenetics 55 (2003) 296–306.
[20] S. Nascimento Diana, et al., Cloning, promoter analysis and expression in response to bacterial exposure of sea bass (Dicentrarchus labrax L.) interleukin-12 p40 and p35 subunits, Mol. Immunol. 44 (9) (2007) 2277–2291.
[21] O. Huising Mark, et al., The presence of multiple and differentially regulated interleukin-12p40 genes in bony fishes signifies an expansion of the vertebrate heterodimeric cytokine family, Mol. Immunol. 43 (10) (2006) 1519–1533.
[22] A. Larkin Mark, et al., Clustal W and clustal X version 2.0, Bioinformatics 23 (21) (2007) 2947–2948.
[23] F. Altschul Stephen, et al., Gapped BLAST and PSI-BLAST: a new generation of protein database search programs, Nucleic Acids Res. 25 (17) (1997) 3389–3402.
[24] Christina Yoon, et al., Charged residues dominate a unique interlocking topography in the heterodimeric cytokine interleukin-12, EMBO J. 19 (14) (2000) 3530–3541.
[25] D. Schmittgen Thomas, Kenneth J. Livak, Analyzing real-time PCR data by the comparative CT method, Nat. Protoc. 3 (6) (2008) 1101–1108.
[26] Jui-Ling Tsai, et al., Grouper interleukin-12, linked by an ancient disulfide-bond architecture, exhibits cytokine and chemokine activities, Fish Shellfish Immunol. 36 (1) (2014) 27–37.
[27] Megumi Matsumoto, et al., Identification and functional characterization of multiple interleukin 12 in amberjack (*Seriola dumerili*), Fish Shellfish Immunol. 55 (2016) 281–292.
[28] Jailon Olivier, et al., Genome duplication in the teleost fish *Tetraodon nigroviridis* reveals the early vertebrate proto-karyotype, Nature 431 (2004) 946–957.
[29] Oppmann Birgit, et al., Novel p19 protein engages IL-12p40 to form a cytokine, IL-23, with biological activities similar as well as distinct from IL-12, Immunity 13 (2000) 715–725.
[30] Tiehui Wang, Mansourah Husain, The expanding repertoire of the IL-12 cytokine family in teleost fish: identification of three paralogues each of the p35 and p40 genes in salmonids, and comparative analysis of their expression and modulation in Atlantic salmon *Salmo salar*, Dev. Comp. Immunol. 46 (2014) 194–207.
[31] Kondera Elzbieta, Witeska Malgorzata, Cadmium and copper reduce hematopoietic

potential in common carp (*Cyprinus carpio* L.) head kidney, Fish Physiol. Biochem. 39 (2013) 755–764.
[32] Wysocka Maria, et al., Interleukin-12 is required for interferon-γ production and lethality in lipopolysaccharide-induced shock in mice, Eur. J. Immunol. 25 (1995) 672–676.
[33] Kubin Marek, M. Chow Janet, Giorgio Trinchieri, Differential regulation of interleukin-12 (IL-12), tumor necrosis factor α, and IL-1β production in human myeloid leukemia cell lines and peripheral blood mononuclear cells, Blood 83 (7) (1994) 1847–1855.
[34] Marchant Arnaud, et al., Interleukin-10 controls interferon-γ and tumor necrosis factor production during experimental endotoxemia, Eur. J. Immunol. 24 (1994) 1167–1171.
[35] Annalisa D'Andrea, et al., Interleukin 10 (IL-10) inhibits human lymphocyte interferon γ-production by suppressing natural killer cell stimulatory factor/IL-12 synthesis in accessory cells, J. Exp. Med. 178 (1993) 1041–1048.
[36] Chomarat Pascale, et al., Interferon γ inhibits interleukin 10 production by monocytes, J. Exp. Med. 177 (1993) 523–527.
[37] Tiehui Wang, et al., Differential expression, modulation and bioactivity of distinct fish IL-12 isoforms: implication towards the evolution of Th1-like immune responses, Eur. J. Immunol. 44 (2014) 1541–1551.
[38] P. Pandit Narayan, et al., Differential expression of interleukin-12 p35 and p40 subunits in response to *Aeromonas hydrophila* and *Aquareovirus* infection in grass carp, Ctenopharyngodon idella, Genet. Mol. Res. 14 (1) (2015) 1169–1183.
[39] P.T. Mehrotra, et al., Effects of IL-12 on the generation of cytotoxic activity in human CD8+ T lymphocytes, J. Immunol. 151 (1993) 2444–2452.
[40] R. Lauwerys Bernard, et al., Cytokine production and killer activity of NK/T-NK cells derived with IL-2, IL-15, or the combination of IL-12 and IL-18, J. Immunol. 165 (2000) 1847–1853.
[41] C. Lili, et al., Contribution of interleukin-12p35 (IL-12p35) and IL-12p40 to protective immunity and pathology in mice infected with *Chlamydia muridarum*, Infect. Immun. 81 (8) (2013) 2962–2971.